

# He II optical depth and UV escape fraction of galaxies

Vikram Khaire\* and Raghunathan Srianand

*IUCAA, Post Bag 4, Pune, India - 411007*

Accepted for publication in MNRAS Letters on 2013 January 17

## ABSTRACT

We study the effect of H I ionizing photons escaping from high-redshift (high- $z$ ) galaxies have on the He II ionizing ultraviolet background (UVB) radiation. While these photons do not directly interact with He II ions, we show that they play an important role, through radiative transport, in modifying the shape of He II ionizing part of UVB spectrum. Within the observed range of UV escape from galaxies, we show that the rapid increase in He II Ly $\alpha$  effective optical depth at  $z \sim 2.7$  can naturally be explained by radiative transport effects. Therefore, the relationship between a well measured He II Ly  $\alpha$  effective optical depth and the redshift in the post-He II reionization era can be used to place additional constraints on the redshift evolution of UV escape from high- $z$  galaxies. Our study also suggests that the escape fraction of H I ionizing photons from galaxies has an important role in the fluctuations of the He II ionizing UVB.

**Key words:** Intergalactic medium–cosmology: theory–diffuse radiation.

## 1 INTRODUCTION

The spectroscopy of  $z \geq 6$  quasi-stellar objects (QSOs; Fan et al. 2006) and cosmic microwave background (CMB) polarization observations (Larson et al. 2011) suggest that H I in the intergalactic medium (IGM) became reionized at  $6 \leq z \leq 12$ . The reionized IGM at  $z \leq 6$  is believed to be in ionization equilibrium with the ultraviolet background (UVB) emanating from QSOs and galaxies (Haardt & Madau 2012, HM12 hereafter). The measured temperature of the IGM at  $z \leq 3$  (Becker et al. 2011), the claimed excess temperature around  $z \sim 6$  QSOs (Bolton et al. 2012), the lack of substantial contribution to  $E > 54.4$  eV photons from galaxies and the redshift distribution of QSOs (Hopkins et al. 2007) all favor He II reionization occurs in the range  $2.5 \leq z \leq 6.0$ .

Direct measurements of He II Lyman  $\alpha$  (Ly $\alpha$ ) absorption from the IGM is possible towards few UV bright high- $z$  QSOs using the *Hubble Space Telescope* (for summary of observations, see Shull et al. 2010). The cosmic-variance limited available data suggest a rapid evolution of the He II Ly- $\alpha$  effective optical depth ( $\tau_{\alpha, \text{HeII}}$ ) and a large fluctuation in the column density ratio of He II and H I (called  $\eta$ ) in the range  $2.7 \leq z \leq 3.0$ . The rapid evolution of the  $\tau_{\alpha, \text{HeII}}$  is attributed to the completion of He II reionization at this epoch (Furlanetto & Oh 2008; McQuinn et al. 2009). The large fluctuation in  $\eta$  over small scales can be attributed to the following: (i) the small number of bright QSOs within a typical mean free path ( $\lambda_{\text{mfp}}$ ) of He II ionizing photons

(Fardal et al. 1998; Furlanetto 2009); (ii) the large scatter in the QSO spectral index (Shull et al. 2004); (iii) the presence of collisionally ionized gas (Muzahid et al. 2011); (iv) the small scale radiative transport effects (Maselli & Ferrara 2005). Most theoretical calculations of the He II optical depth have considered only the QSO emissivity and radiative transport, assuming that the IGM gas in photoionization equilibrium. While galaxies do not contribute directly to the He II ionizing radiation, they can influence the ionization state of the IGM gas, thereby affecting the He II optical depth. Here, we explore this issue, using a cosmological radiative transfer code similar to HM12 keeping the galaxy contribution as a free parameter within the range allowed by the observations. We show that  $\lambda_{\text{mfp}}$  is very sensitive to the escape fraction ( $f_{\text{esc}}$ ) of H I ionizing photons from galaxies. In Section 2, we provide details of our calculations assuming a  $(\Omega_m, \Omega_\Lambda, h) = (0.3, 0.7, 0.7)$  cosmology.

## 2 UVB CALCULATION

We have calculated the UVB spectrum contributed by QSOs and galaxies using the standard assumption that each volume element is an isotropic emitter and sink (e.g. Haardt & Madau 1996; Fardal et al. 1998; Faucher-Giguère et al. 2009). The angle and space averaged specific intensity  $J_{\nu_0}$  (in units of  $\text{erg cm}^{-2} \text{s}^{-1} \text{Hz}^{-1} \text{sr}^{-1}$ ) of diffuse UVB, as seen by an observer at a redshift  $z_0$  and frequency  $\nu_0$  is given by (Haardt & Madau 1996):

$$J_{\nu_0}(z_0) = \frac{1}{4\pi} \int_{z_0}^{\infty} dz \frac{dl}{dz} \frac{(1+z_0)^3}{(1+z)^3} \epsilon_{\nu}(z) e^{-\tau_{\text{eff}}(\nu_0, z_0, z)}. \quad (1)$$

\* E-mail: vikramk@iucaa.ernet.in

Here,  $\nu = \nu_0(1+z)/(1+z_0)$  is the frequency of emitted radiation at redshift  $z$ ,  $\epsilon_\nu(z)$  is the proper space-averaged specific volume emissivity of radiating sources (QSOs and galaxies),  $\frac{dl}{dz}$  is the proper line element in the Friedmann-Robertson-Walker cosmology and  $\tau_{\text{eff}}$  is the effective optical depth, which quantifies the attenuation of photons observed at a frequency  $\nu_0$  while travelling through the IGM in between  $z$  and  $z_0$ .

If we assume that the IGM clouds with neutral hydrogen column density,  $N_{\text{HI}}$ , are Poisson-distributed along the line of sight, we can write  $\tau_{\text{eff}}$  as (Paresce et al. 1980),

$$\tau_{\text{eff}}(\nu_0, z_0, z) = \int_{z_0}^z dz' \int_0^\infty dN_{\text{HI}} \frac{\partial^2 N}{\partial N_{\text{HI}} \partial z'} [1 - e^{-\tau(\nu')}] . \quad (2)$$

Here,  $f(N_{\text{HI}}, z) = \partial^2 N / \partial N_{\text{HI}} \partial z$ , is the number of absorbers with  $N_{\text{HI}}$  per unit redshift and column density interval measured at  $z$ . This is directly measured with QSO spectroscopy (see Petitjean et al. 1993). Assuming that absorbing clouds are made up of a pure H and He gas, the continuum optical depth through an individual cloud can be written as

$$\tau(\nu') = N_{\text{HI}} \sigma_{\text{HI}}(\nu') + N_{\text{HeI}} \sigma_{\text{HeI}}(\nu') + N_{\text{HeII}} \sigma_{\text{HeII}}(\nu') . \quad (3)$$

Here,  $\nu' = \nu_0(1+z')/(1+z_0)$  and  $N_x$  and  $\sigma_x$  are the column density and photoionization cross-section for a species  $x$ , respectively. From QSO spectroscopy, we know that  $N_{\text{HeI}}$  is negligible when  $N_{\text{HI}} \leq 10^{17.2} \text{ cm}^{-2}$ . Even for Lyman limit systems ( $N_{\text{HI}} > 10^{17.2} \text{ cm}^{-2}$ ), the ratio  $N_{\text{HeI}}/N_{\text{HI}}$  is small (see HM12) enough to neglect its contribution over the redshift range of interest in our study. Therefore, Eq. (3) becomes

$$\tau(\nu) \approx N_{\text{HI}} [\sigma_{\text{HI}}(\nu) + \eta \sigma_{\text{HeII}}(\nu)] . \quad (4)$$

In the absence of direct measurements of  $f(N_{\text{HeII}}, z)$ , a knowledge of  $\eta$  as a function of  $N_{\text{HI}}$  together with  $f(N_{\text{HI}}, z)$  allows us to calculate the contribution of He II to the continuum optical depth. Under photoionization equilibrium,  $N_{\text{HI}}$  and  $N_{\text{HeII}}$  are related through the following quadratic equation (Fardal et al. 1998; Faucher-Giguère et al. 2009; Haardt & Madau 2012):

$$\frac{n_{\text{He}}}{4n_{\text{H}}} \frac{I_{\text{HI}} \tau_{912, \text{HI}}}{(1+A \tau_{912, \text{HI}})} = \tau_{228, \text{HeII}} + \frac{I_{\text{HeII}} \tau_{228, \text{HeII}}}{(1+B \tau_{228, \text{HeII}})} . \quad (5)$$

Here,  $\tau_{\lambda, x}$  is  $N_x \sigma_x(\lambda)$  for the species  $x$ . The values of A and B depend on the assumed relationship between the total hydrogen column density ( $N_{\text{H}}$ ) and electron density ( $n_e$ ). This relationship is obtained for a constant density slab of gas with a thickness of Jeans length under optically thin photoionization equilibrium (Schaye 2001). Numerical simulations suggest that such a relationship is valid for  $\log N_{\text{H}} \leq 18$  (see Rahmati et al. 2012). We have considered a series of photoionization models of plane parallel slab having  $N_{\text{H}}-n_e$  relationship of Schaye (2001) illuminated by a power law source using the photoionization code CLOUDY (see Ferland et al. 1998). We confirm that the values A = 0.02 and B = 0.25 (as used by HM12) provide a good fit to the model predictions, and adopt these values in our calculations. The quantity  $I_x$  for the  $x^{\text{th}}$  species is defined as  $I_x = \Gamma_x / n_e \alpha_x(T)$ , where  $\alpha_x(T)$  is the case-A recombination coefficient and  $\Gamma_x$  is photoionization rate of  $x^{\text{th}}$

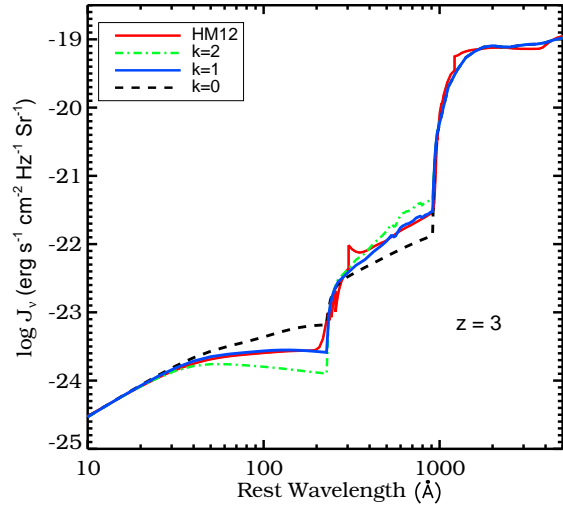


**Figure 1.** UV background spectrum at  $z = 3$  from our models for different values of  $k$ . The spectrum plotted in red is from HM12.

species as given by,

$$\Gamma_x = \int_{\nu_x}^\infty d\nu 4\pi \frac{J_\nu}{h\nu} \sigma_x(\nu) . \quad (6)$$

Here,  $\nu_x$  is the ionization threshold frequency for the species  $x$ . In all our calculations, we use  $T = 2 \times 10^4 \text{ K}$  and the form of  $n_e$  and  $f(N_{\text{HI}}, z)$  as given by HM12.

## 2.1 Quasar and galaxy emissivity

The specific volume emissivity of radiating sources,  $\epsilon_\nu(z)$ , is a sum of the emissivity from galaxies,  $\epsilon_{\nu, \text{G}}(z)$ , and quasars,  $\epsilon_{\nu, \text{Q}}(z)$ . We have considered the parametric form to the observed quasar co-moving emissivity at  $912\text{\AA}$ , as given in HM12,

$$\frac{\epsilon_{912, \text{Q}}(z)}{(1+z)^3} = 10^{24.6} (1+z)^{4.68} \frac{\exp(-0.28z)}{\exp(1.77z) + 26.3} \quad (7)$$

in units of  $\text{ergs Mpc}^{-3} \text{ s}^{-1} \text{ Hz}^{-1}$ , together with the broken power law spectral energy distribution (SED),  $L_\nu \propto \nu^{-0.44}$  for  $\lambda > 1300\text{\AA}$  and  $L_\nu \propto \nu^{-1.57}$  for  $\lambda < 1300\text{\AA}$  (Vanden Berk et al. 2001; Telfer et al. 2002). To calculate the co-moving emissivity from galaxies we have taken the parametric form of star formation rate density (SFRD) used by HM12:

$$\text{SFRD}(z) = \frac{6.9 \times 10^{-3} + 0.14(z/2.2)^{1.5}}{1 + (z/2.7)^{4.1}} \text{ M}_\odot \text{ yr}^{-1} \text{ Mpc}^{-3} . \quad (8)$$

The co-moving emissivity of galaxies (in units  $\text{ergs Mpc}^{-3} \text{ s}^{-1} \text{ Hz}^{-1}$ ) is taken to be,

$$\frac{\epsilon_{\nu, \text{G}}(z)}{(1+z)^3} = C(z) \times \text{SFRD}(z) \times l_\nu(z, Z) . \quad (9)$$

Here,  $l_\nu(z, Z)$  is the specific luminosity of a galaxy produced for every solar mass of gas having metallicity  $Z$  being converted to stars. We obtain  $l_\nu(z, Z)$  using the stellar population synthesis model ‘STARBURST99 v6.0.3’ (Leitherer et al. 1999) for  $Z=0.001$  and Salpeter initial mass function with stellar mass range 0.1 to 100

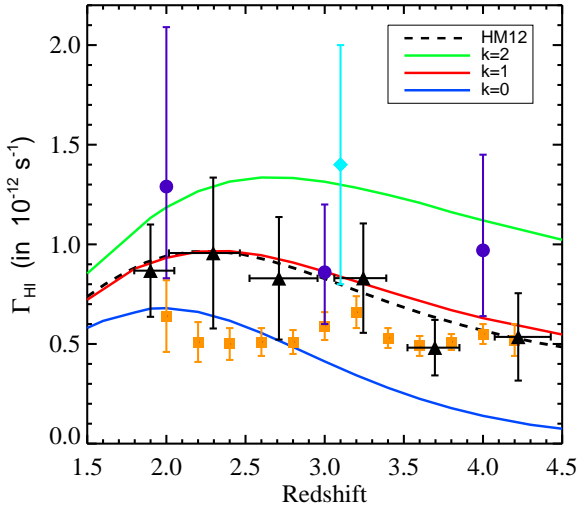


**Figure 2.**  $\Gamma_{\text{HI}}$  vs  $z$  for  $k=0$  to 2. *Squares*: Faucher-Giguère et al. (2008). *Triangles*: Becker et al. (2007) (lognormal model). *Circles*: Bolton & Haehnelt (2007). *Diamond*: Nestor et al. (2012).

$M_{\odot}$ . SED fitting studies, semi-analytic modeling of luminosity function and spatial clustering are consistent with star formation in a typical galaxy lasting for a few 100 Myr (see discussions in Jose et al. 2012, and references therein). Therefore, for simplicity, we assume that the star formation has lasted for more than 100 Myr. This assumption allows us to get a linear relationship between the star formation rate and luminosity. We confirm that  $\epsilon_{912,G}$ , obtained using this assumption, is consistent with the one using convolution integral (equation 55 of HM12). We do not include recombination emissivity and resonant absorption effects in our calculations.

The factor  $C(z)$  is used to modify the SED in order to take care of the reddening and UV escape. For  $\lambda > 912\text{\AA}$ ,  $C(z)$  is  $\exp(-\tau_{\nu})$  with  $\tau_{\nu}$  being the frequency-dependent dust optical depth, calculated using extinction law of Calzetti et al. (2000) with  $R_V = 3.1$ . The dust correction might depend on the luminosity and  $z$  of individual galaxies (see for example Bouwens et al. 2012). However, for simplicity, we use a single value at all values of  $z$ . The dust optical depth is chosen to have a reddening correction factor of 3 at  $1500\text{\AA}$ .

For wavelength range  $228\text{\AA} < \lambda < 912\text{\AA}$  we take  $C(z) = f_{\text{esc}}$ . To take into account the redshift evolution in the  $f_{\text{esc}}$  found by Inoue et al. (2006), we adopt the form of HM12 and use

$$C(z) = f_{\text{esc}} = k [3.4 \times 10^{-4} (1+z)^{3.4}]. \quad (10)$$

In this case,  $C(z)$  corresponds to the absolute escape fraction,  $f_{\text{esc}}$ , defined as the ratio of escaping Lyman continuum (LyC) flux from a galaxy to the one which is intrinsically produced by the stars in it (Leitherer et al. 1995), and  $k$  is a free parameter that allows us to change the values of  $f_{\text{esc}}$ . For our fiducial star formation model, at  $k=1$ , we obtain UV emissivity from galaxies similar to that of HM12. The model with  $k=0$  corresponds to spectrum contributed by QSOs alone at  $\lambda < 912\text{\AA}$ . Note that no reddening correction is applied for  $\lambda < 912\text{\AA}$  and we simply scale the unattenuated

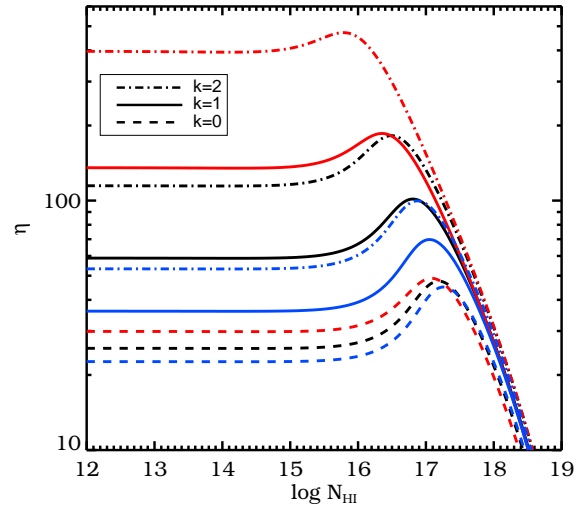


**Figure 3.**  $\eta$  as a function of  $N_{\text{HI}}$  for redshifts 2 (blue), 2.5 (black) and 3 (red). The dash, solid and dot-dash curves are for  $k = 0, 1$  and 2 respectively.

spectrum by  $f_{\text{esc}}$ . In other words, we assume that the ionizing photons that are escaping through holes in the galaxy. We take  $C(z) = 0$  for  $\lambda < 228\text{\AA}$  because galaxies at the redshifts in which we are interested do not produce sufficient He II ionizing photons because massive Population-III stars are rare.

### 3 RESULTS AND DISCUSSION

In Fig. 1, we present the UVB spectrum at  $z=3$  computed using our numerical code for three different values of  $k$ . At  $z=3$ ,  $k=1$  and 2 corresponds to  $f_{\text{esc}} \sim 4\%$  and  $\sim 8\%$ , respectively. This is well within the inferred range for high- $z$  galaxies and Ly- $\alpha$  emitters at  $z \sim 3$  (Shapley et al. 2006; Iwata et al. 2009; Boutsia et al. 2011; Nestor et al. 2012). The range of  $\Gamma_{-12,\text{HI}} = 0.4 - 1.3$  predicted by our models is also consistent with the range allowed by the observations (see Fig. 2). For comparison, in Fig. 1, we also plot the UVB spectrum generated by HM12. It is clear that our model with  $k=1$  reproduces HM12 spectrum very well. The differences in  $\Gamma_{\text{HI}}$  and  $\Gamma_{\text{HeII}}$  between the two codes is much less than the spread in these values because of the allowed range in  $f_{\text{esc}}$ . It is clear from Fig. 1 that increasing (decreasing)  $k$  increases (decreases)  $\Gamma_{\text{HI}}$  and decreases (increases)  $\Gamma_{\text{HeII}}$ . Because  $\lambda \leq 228\text{\AA}$  emissivity is not affected by galaxies, the variation of  $\Gamma_{\text{HeII}}$  with  $f_{\text{esc}}$  can be attributed to the effect of  $f_{\text{esc}}$  on He II opacity. Here, we explore this in more detail.

#### 3.1 Escape fraction and $\eta$

In Fig. 3, we plot  $\eta$  versus  $N_{\text{HI}}$  at redshift 2, 2.5 and 3 for different values of  $k$ . Two trends are clearly evident for  $\log(N_{\text{HI}}) \leq 17$ : (i) for any given  $f_{\text{esc}}$ ,  $\eta$  increases with increasing  $z$  and (ii) at any  $z$ ,  $\eta$  increases with increasing  $f_{\text{esc}}$ . The first trend can be understood in a simple way for the optically thin limit where  $\eta \propto \Gamma_{\text{HI}}/\Gamma_{\text{HeII}}$ . Both

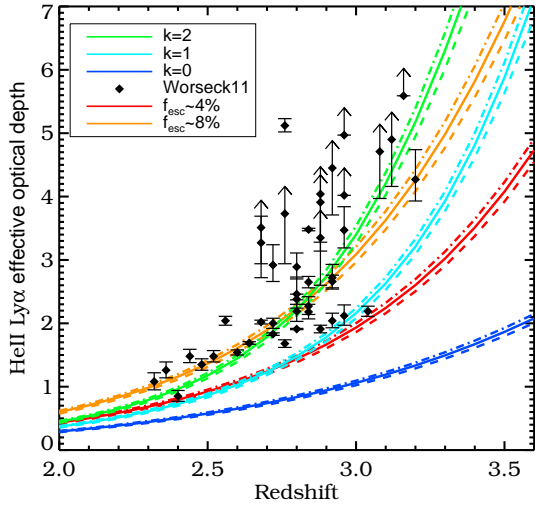


**Figure 4.** Ly $\alpha$  effective optical depth for He II as a function of redshift for different  $f_{\text{esc}}$  and  $b$  parameters ( $b = 28$  dash curve,  $b = 30$  solid curve,  $b = 32$  dot dash curve in km/s). Black diamonds are observations of Worseck et al. (2011).

QSOs and galaxies contribute to  $\Gamma_{\text{HI}}$  but only QSOs contribute to  $\Gamma_{\text{HeII}}$ . Therefore,  $\eta$  depends on how the population of QSOs and galaxies evolve with redshift. For  $z \geq 2.5$ , the population of QSOs declines rapidly (Ross et al. 2012), while that of galaxies remains almost the same (Bouwens et al. 2011), which helps  $\eta$  to increase. However, at any  $z$ , by increasing  $f_{\text{esc}}$ , we are increasing the galaxy contribution to  $\Gamma_{\text{HI}}$ , which will further increase  $\eta$ . This explains the second trend that we notice in Fig. 3. *We can draw a simple physical picture: a given  $N_{\text{HI}}$  is produced by integrating over a larger column length when  $\Gamma_{\text{HI}}$  is high, and therefore we obtain more  $N_{\text{HeII}}$ .* However, the effects which we discuss here are obtained by keeping  $\Gamma_{\text{HI}}$  well within the range allowed by the existing observations (see Fig. 2).

### 3.2 Ly $\alpha$ effective optical depth for H I and He II

Now, we estimate the Ly  $\alpha$  effective optical depth of H I (i.e.,  $\tau_{\alpha,\text{HI}}$ ) and He II (i.e.,  $\tau_{\alpha,\text{HeII}}$ ) for a range of  $f_{\text{esc}}$ , and we compare the results with the available observations. The  $\tau_{\alpha,\text{HI}}$  and  $\tau_{\alpha,\text{HeII}}$  are given by (Paresce et al. 1980; Madau & Meiksin 1994),

$$\tau_{\alpha,x}(z) = \frac{1+z}{\lambda_{\alpha,x}} \int_0^\infty dN_{\text{HI}} f(N_{\text{HI}}, z) W_n, \quad (11)$$

where,  $\lambda_{\alpha,x}$  is 1215.67Å for H I, 303.78Å for He II. Here,  $W_n$  is the equivalent width of corresponding line, expressed in wavelength units, given by

$$W_n = \int_0^\infty d\lambda (1 - e^{-y\phi(\lambda)}), \quad (12)$$

where  $y = N_{\text{HI}}$  for H I,  $y = \eta N_{\text{HI}}$  for He II and  $\phi(\lambda)$  is Voigt profile function. We find that the observed relationship between  $\tau_{\alpha,\text{HI}}$  and  $z$  (Becker et al. 2012) is well reproduced if we use  $b$  parameter values  $b = 30 \pm 2$   $\text{kms}^{-1}$ .

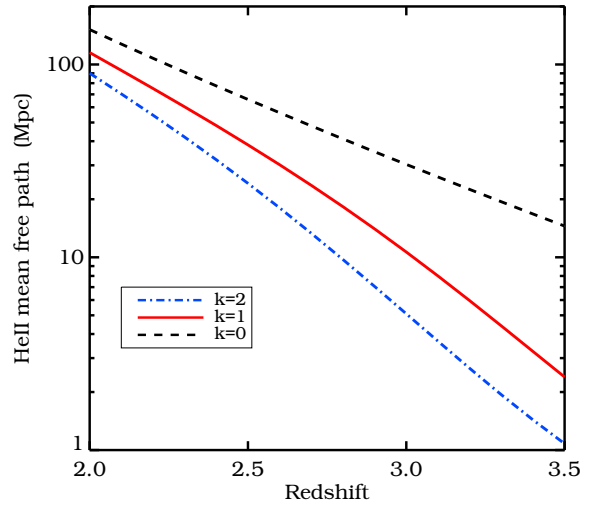


**Figure 5.** Mean free path for He II ionizing photons as a function of  $z$  for different  $k$  values. Here, distance is in proper length scale.

In Fig. 4, we plot  $\tau_{\alpha,\text{HeII}}$  versus  $z$  for different values of  $f_{\text{esc}}$ , along with observations of Worseck et al. (2011). Here, we assume that the non-thermal motions dominate the He II line broadening and used the best-fitting values of  $b$  obtained for H I. In all cases  $\tau_{\alpha,\text{HeII}}$  increases with increasing  $z$ . However the rate of increase depends on  $f_{\text{esc}}$ . Interestingly, the sharp raising trend of  $\tau_{\alpha,\text{HeII}}$  at  $z \sim 3$ , seen for  $k=1$ , almost provides a lower envelop to the observations. For  $k=2$ , the model prediction almost passes through most of the observed mean points at  $z \leq 2.7$ . This means that  $f_{\text{esc}}$  can not be much higher than 8% in this redshift range. To check whether the rapid rise in  $\tau_{\alpha,\text{HeII}}$  is a consequence of the  $(1+z)^{3,4}$  evolution assumed for  $f_{\text{esc}}$  (Eq. 10), in Fig.4 we also plot the  $\tau_{\alpha,\text{HeII}}$  computed for redshift-independent  $f_{\text{esc}}$  (i.e. 4% and 8%). Even in these cases, the  $z$  evolution of  $\tau_{\alpha,\text{HeII}}$  is steeper than for  $k=0$ . This observed rise and scatter in  $\tau_{\alpha,\text{HeII}}$  is usually attributed to the pre-overlap era of He III bubbles, assuming that the He II re-ionization completes around  $z = 2.7$  (Dixon & Furlanetto 2009; Shull et al. 2010; Worseck et al. 2011). *Our results suggest that the observed trend of  $\tau_{\alpha,\text{HeII}}$  with  $z$  can also be produced naturally by the radiative transfer effects associated with changing  $f_{\text{esc}}$ .*

Next, we calculate the  $\lambda_{\text{mpf}}$  predicted by our models. We define,

$$\lambda_{\text{mpf}} = \left| \frac{dl}{dz} \right| \frac{dz}{d\tau_{\text{eff}}}, \quad (13)$$

where, from Eq. (2), we write,

$$\frac{d\tau_{\text{eff}}}{dz} = \int_0^\infty dN_{\text{HI}} f(N_{\text{HI}}, z) [1 - e^{-\tau(228\text{\AA})}]. \quad (14)$$

Here,  $\tau(228\text{\AA}) = N_{\text{HI}}(\sigma_{\text{HI},228\text{\AA}} + \eta\sigma_{\text{HeII},228\text{\AA}})$ . In Fig. 5,  $\lambda_{\text{mpf}}$  of He II ionizing photons is plotted as a function of  $z$  for different values of  $f_{\text{esc}}$ . These curves are well approximated by  $\lambda_{\text{mpf}}(z) = A_1 \times \exp[-(z-2)/\Delta z]$  with best-fitting values of  $A_1 = [150, 120, 90]$  Mpc and  $\Delta z = [0.60, 0.41, 0.37]$ , respectively, for  $k = [0, 1, 2]$ . This clearly demonstrates the rapid reduction in  $\lambda_{\text{mpf}}$  with  $f_{\text{esc}}$ . This is a consequence of the fact

that when we increase  $f_{\text{esc}}$ , a given  $N_{\text{HeII}}$  is produced by a cloud with lower  $N_{\text{HI}}$  (i.e.  $\eta$  increases). Because  $f(N_{\text{HI}}, z)$  is a powerlaw in  $N_{\text{HI}}$  with a negative slope,  $\lambda_{\text{mfp}}$  reduces steeply. For our fiducial model with  $k=1$ ,  $\lambda_{\text{mfp}}$  is 22 and 11 proper Mpc at  $z=2.7$  and 3.0, respectively. These values are at least a factor 2 smaller than the corresponding values for  $k=0$ .

Recently, Davies & Furlanetto (2012) have computed the mean evolution of  $\tau_{\alpha, \text{HeII}}$ , assuming diffuse emissivity of QSOs and allowing for fluctuating  $\Gamma_{\text{HeII}}$ . This model also produces a rapidly evolving  $\tau_{\alpha, \text{HeII}}$  with  $z$  without implicitly assuming He II reionization around  $z \sim 3$ , when a minimum  $\lambda_{\text{mfp}}$  of 35 comoving Mpc is used. This is already more than  $\lambda_{\text{mfp}}$  we obtain at  $z = 3$  for our fiducial model. Therefore, we can conclude that  $f_{\text{esc}}$  will play an important role in the calculations of the fluctuation. We also speculate that the redshift at which the fluctuations begin to dominate will depend on  $f_{\text{esc}}$ . Detailed investigations of high ionization species, such as N V and O VI absorption in QSO spectra at  $z \geq 2.5$ , and proximity effect analysis of He II Ly- $\alpha$  forest will provide more insights into the issues discussed here. We plan to address these topics carefully in the near future.

#### 4 CONCLUSIONS

We have studied the effect of escape fraction of H I ionizing photons from high- $z$  galaxies on the UVB, calculated by solving cosmological radiative transfer equation. We have demonstrated that H I ionizing photons from galaxies play an important role in deciding the shape of He II ionizing part of UVB and that they affect the transmission of the UVB through the IGM. Here, we summarize our main results.

(i) The He II ionizing part of UVB depends greatly on the value of  $f_{\text{esc}}$  for  $z > 2.0$ . This is a consequence of the dependence of ratio  $\eta = N_{\text{HeII}}/N_{\text{HI}}$  on  $f_{\text{esc}}$ .

(ii) Mean free path of He II ionizing photons decreases rapidly with increasing  $f_{\text{esc}}$ , which suggests that it will play an important role in quantifying the fluctuations in He II ionizing UVB.

(iii) We show that, for the range of  $f_{\text{esc}}$  allowed by the observations, the rapid increase in He II Ly $\alpha$  effective optical depth (recently observed at  $z \sim 2.7$ ) can be explained naturally. In the literature such a trend is attributed to the pre-overlap era of He III bubbles, assuming that the He II re-ionization completes around  $z = 2.7$ . Our study, while providing an alternate explanation, does not rule out this possibility. However, we show that it will be possible to place additional constraints on  $f_{\text{esc}}$  in the post-He II reionization era using well measured He II Ly $\alpha$  effective optical depths. We also show that the observations at  $z \leq 2.7$  are consistent with the fact that  $f_{\text{esc}}$  is not much higher than 8%.

#### ACKNOWLEDGMENTS

We wish to thank T. R. Choudhury, K. Subramanian and the referee for useful suggestions. VK thanks CSIR for providing support for this work.

#### REFERENCES

- Becker G. D., Rauch M., Sargent W. L. W., 2007, ApJ, 662, 72
- Becker G. D., Bolton J. S., Haehnelt M. G., Sargent W. L. W., 2011, MNRAS, 410, 1096
- Becker G. D., Hewett P. C., Worseck G., Prochaska J. X., 2012, MNRAS, in press, (arXiv:1208.2584)
- Bolton J. S., Haehnelt M. G., 2007, MNRAS, 382, 325
- Bolton J. S., Becker G. D., Raskutti S., Wyithe J. S. B., Haehnelt M. G., Sargent W. L. W., 2012, MNRAS, 419, 2880
- Boutsia K. et al., 2011, ApJ, 736, 41
- Bouwens R. J. et al., 2011, Natur, 469, 504
- Bouwens R. J. et al., 2012, ApJ, 754, 83
- Calzetti D., Armus L., Bohlin R. C., Kinney A. L., Koornneef J., Storchi-Bergmann T., 2000, ApJ, 533, 682
- Davies F. B., Furlanetto S. R., 2012, ArXiv e-prints (arXiv:1209.4900)
- Dixon K. L., Furlanetto S. R., 2009, ApJ, 706, 970
- Fan X. et al., 2006, AJ, 132, 117
- Fardal M. A., Giroux M. L., Shull J. M., 1998, AJ, 115, 2206
- Faucher-Giguère C. A., Prochaska J. X., Lidz A., Hernquist L., Zaldarriaga M., 2008, ApJ, 681, 831
- Faucher-Giguère C. A., Lidz A., Zaldarriaga M., Hernquist L., 2009, ApJ, 703, 1416
- Ferland G. J., Korista K. T., Verner D. A., Ferguson J. W., Kingdon J. B., Verner E. M., 1998, PASP, 110, 761
- Furlanetto S. R., 2009, ApJ, 703, 702
- Furlanetto S. R., Oh S. P., 2008, ApJ, 681, 1
- Haardt F., Madau P., 1996, ApJ, 461, 20
- Haardt F., Madau P., 2012, ApJ, 746, 125 (HM12)
- Hopkins P. F., Richards G. T., Hernquist L., 2007, ApJ, 654, 731
- Inoue A. K., Iwata I., Deharveng J. M., 2006, MNRAS, 371, L1
- Iwata I. et al., 2009, ApJ, 692, 1287
- Jose C., Subramanian K., Srianand R., Samui S., 2013, MNRAS, in press (doi:10.1093/mnras/sts503)
- Larson D. et al., 2011, ApJS, 192, 16
- Leitherer C., Ferguson H. C., Heckman T. M., Lowenthal J. D., 1995, ApJ, 454, L19
- Leitherer C. et al., 1999, ApJS, 123, 3
- Madau P., Meiksin A., 1994, ApJ, 433, L53
- Maselli A., Ferrara A., 2005, MNRAS, 364, 1429
- McQuinn M., Lidz A., Zaldarriaga M., Hernquist L., Hopkins P. F., Dutta S., Faucher-Giguère C. A., 2009, ApJ, 694, 842
- Muzahid S., Srianand R., Petitjean P., 2011, MNRAS, 410, 2193
- Nestor D. B., Shapley A. E., Kornei K. A., Steidel C. C., Siana B., 2012, ApJ, in press (arXiv:1210.2393)

- Paresce F., McKee C. F., Bowyer S., 1980, *ApJ*, 240, 387
- Petitjean P., Webb J. K., Rauch M., Carswell R. F., Lanzetta K., 1993, *MNRAS*, 262, 499
- Rahmati A., Pawlik A. P., Raičević M., Schaye J., 2012, *MNRAS*, in press (arXiv:1210.7808)
- Ross N. P. et al., 2012, *ArXiv e-prints* (arXiv:1210.6389)
- Schaye J., 2001, *ApJ*, 559, 507
- Shapley A. E., Steidel C. C., Pettini M., Adelberger K. L., Erb D. K., 2006, *ApJ*, 651, 688
- Shull J. M., Tumlinson J., Giroux M. L., Kriss G. A., Reimers D., 2004, *ApJ*, 600, 570
- Shull J. M., France K., Danforth C. W., Smith B., Tumlinson J., 2010, *ApJ*, 722, 1312
- Telfer R. C., Zheng W., Kriss G. A., Davidsen A. F., 2002, *ApJ*, 565, 773
- Vanden Berk D. E. et al., 2001, *AJ*, 122, 549
- Worseck G. et al., 2011, *ApJ*, 733, L24